
MADNET: USING A MAD OPTIMIZATION FOR DEFENDING AGAINST ADVERSARIAL ATTACKS

Shai Rozenberg

Technion – Israel Institute of Technology
shairoz@cs.technion.ac.il

Gal Elidan

Google Research
elidan@google.com

Ran El-Yaniv

Technion
rani@cs.technion.ac.il

ABSTRACT

This paper is concerned with the defense of deep models against adversarial attacks. Inspired by the certificate defense approach, we propose a maximal adversarial distortion (MAD) optimization method for robustifying deep networks. MAD captures the idea of increasing separability of class clusters in the embedding space while decreasing the network sensitivity to small distortions. Given a deep neural network (DNN) for a classification problem, an application of MAD optimization results in MadNet, a version of the original network, now equipped with an adversarial defense mechanism. MAD optimization is intuitive, effective and scalable, and the resulting MadNet can improve the original accuracy. We present an extensive empirical study demonstrating that MadNet improves adversarial robustness performance compared to state-of-the-art methods.

1 Introduction

Defending machine learning models from adversarial attacks has become an increasingly pressing issue as deep neural networks (DNNs) are utilized in evermore facets of daily life. Adversarial attacks can effectively fool deep models and force them to misclassify, using a slight but maliciously-designed distortion that, in the image domain, is typically invisible to the human eye Szegedy et al. [2013], Goodfellow et al. [2014], Kurakin et al. [2016a], Carlini and Wagner [2017b], Athalye et al. [2018]. Despite the advances in protecting against such attacks (see Section 4), defense mechanisms are still wanting.

In this paper we study adversarial attacks through the lens of class activation geometry in embedding layers. We observe that a trained deep classification model tends to organize instances into clusters in the embedding space, according to class labels. Classes with clusters in close proximity to one another provide excellent opportunities for attackers to fool the model. This activation geometry explains the tendency of untargeted attacks to alter the label of, for example, a given image to that of an adjacent class in the embedding space. This observation is illustrated in Figure 1 as follows. We trained Resnet-56 He et al. [2016] over the CIFAR-10 Krizhevsky and Hinton [2009] image dataset and calculated the class centroids, computed using the L_2 mean of class embeddings (pre-logits activation). Figure 1a depicts in colors the distances between class centroids. For instance, the closest class to *truck* is *automobile* and the closest class to *dog* is *cat*. We then attacked this network using the C&W (untargeted) attack Carlini and Wagner [2017a], and generated many adversarial examples. Figure 1b depicts the class confusion matrix of this ResNet obtained by classifying the adversarial instances. We see, for example, that images from class *truck* tend to be adversarially perturbed so that they are classified as *automobile*, as indicated by the red matrix cell, indicating a frequent label change between these classes. Similarly, classes *dog* is classified as *cat*, also a frequent misclassification as a result of this attack. The Euclidean distance provides only partial information about the identity of the adversarial class. In untargeted attacks in which the attacker creates an adversarial example with no constraints on the adversarial class, performs a “step” in the direction of the gradient. As such, the qualitative nature of the observation.

Such cluster geometry observations intuitively suggest that, by increasing the margin between clusters, we could make the network more immune to attacks without compromising accuracy. Indeed manifestations of similar concepts have already been considered in the context of large margin classification and generalization capabilities Sun et al. [2016], Liang et al. [2017], Sokolić et al. [2017].

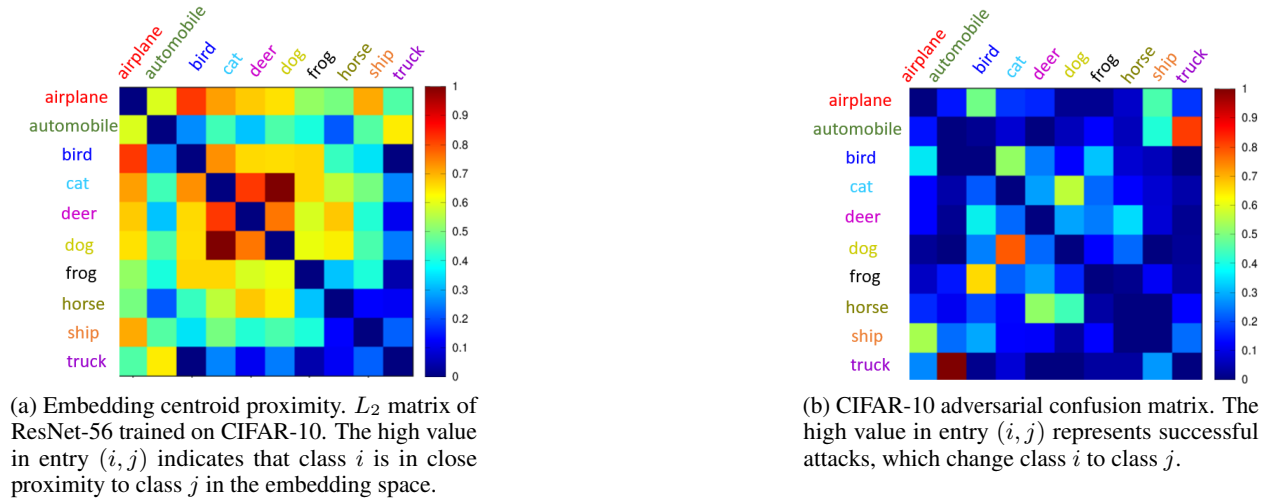


Figure 1: CIFAR-10: DNN embedding distance matrix and C&W adversarial confusion matrix.

Here we present an adversarial defense method that captures the notion of increased separability in embedding space. While increased separability motivations for defense methods appeared elsewhere Mustafa et al. [2019], the crux in our method is that distances must be normalized by the network sensitivity in order to be meaningful. Otherwise, one may get a false sense of separability in the embedding space with a network that travels large distances in this space in response to tiny changes in the input space. This sensitivity can be quantified through a Lipschitz constant, or directly via the Jacobian of the embedding layer with respect to the input.

Using a distortion ϵ , the adversary tried to compel a DNN F to misclassify $x + \epsilon$, where x is an input. Ideal, we want to maximize the ϵ needed for this to succeed so that the adversary will fail when using a subtle attack. Using first-order considerations, we propose an approximate lower bound on the effective distortion required by the adversary, which motivates a useful strategy for adding a defense mechanism to any architecture. The first order bound, $\epsilon \geq \eta(F) / \|J_F(x)\|$, which is similar to other known bounds Tsuzuku et al. [2018], is given in terms of $\eta(F)$, the “embedding margin” of the network F , and $J_F(x)$, the Jacobian of F with respect to x (see details in Section 2). The embedding margin, for a given intermediate layer, is the minimum distance between two instances belonging to two different classes. This relation, which we call the *maximal adversarial distortion* (MAD) principle, motivates a MAD optimization technique comprising a loss function and a training routine that maximizes this lower bound without attempting to calculate it. While a large margin is intuitively a useful property that is widely accepted as an inducer of robust classification Hoffer and Ailon [2015], Liu et al. [2016], Wen et al. [2016], the above relation emphasizes the principle that the margin should be measured in terms of gradient of the model with respect to the input. Otherwise, a large margin would be meaningless when small changes to the input correspond to large distances in the embedding space.

To actualize the MAD approach, we introduce two procedures: one to increase the embedding margin, and another for reducing the Jacobian. The margin is increased by both proxying and penalizing the in-between cluster distance using the angular distance, and by explicitly penalizing within-cluster variance. The Jacobian is handled explicitly by penalizing large embedding Jacobian norms. Both procedures are encapsulated in a single MAD optimization procedure, using a Siamese-like training procedure. We refer to a network trained with the MAD optimization as MadNet. An extensive empirical study of MadNet shows results under various threat models, in which we consider FGSM, BIM, C&W and PGD attacks. Our experimental procedure adheres strictly to the comprehensive evaluation desiderata proposed by Carlini et al. [2019]. The results we present indicate definitively that the proposed defense method substantially improves state-of-the-art detection.

2 Maximal Adversarial Distortion (MAD)

In this section we develop the MAD principle, whose goal is to improve normalized separability between classes in the embedding space. The MAD principle will be utilized in Section 3 to develop the MAD optimization approach (loss function and training procedure). Let F be a neural classifier and let $x \in \mathbb{R}^{h \times w}$ be an instance assumed to have the class label $c = c(x)$. Let $\epsilon \in \mathbb{R}^{h \times w}$ be a vector representing an adversarial distortion for instance x such that the

(successful) adversarial instance is $x_{adv} \triangleq x + \epsilon$ whose label is different from c ; namely, $c_{adv} \triangleq F(x_{adv}) \neq c$. The attacker’s goal is to find the smallest distortion ϵ so that F misclassifies x ,

$$\begin{aligned} \min_{\epsilon} \|\epsilon\| \\ \text{s.t. } F(x + \epsilon) \neq c(x). \end{aligned}$$

For a successful adversarial attack whose distortion is required to be small, in the spirit of Hein and Andriushchenko [2017], Ding et al. [2018], Tsuzuku et al. [2018], Zhang et al. [2019], we approximate a prediction for x_{adv} using the first-order Taylor approximation,

$$F(x_{adv}) = F(x + \epsilon) \stackrel{|\epsilon| \ll 1}{\approx} F(x) + J_F(x)\epsilon,$$

which is applied here for tensor-valued functions with $J_F(x)$ being the Jacobian of F . The same approximation applies to the output of any intermediate layer ℓ . Denoting by $F_\ell(x)$ the output of layer ℓ , we have,

$$F_\ell(x_{adv}) \approx F_\ell(x) + J_\ell(x)\epsilon.$$

Taking the Frobenius norm, we get,

$$\|J_\ell(x)\epsilon\| \approx \|F_\ell(x) - F_\ell(x_{adv})\|.$$

The Frobenius norm is sub-multiplicative (proof can be found in Appendix A) so that

$$\|J_\ell(x)\| \|\epsilon\| \geq \|J_\ell(x)\epsilon\| \approx \|F_\ell(x) - F_\ell(x_{adv})\|. \quad (1)$$

For layer ℓ in F , we thus define its *embedding margin*,

$$\eta_\ell(F) \triangleq \arg \min_{x_1, x_2, c(x_1) \neq c(x_2)} \|F_\ell(x_1) - F_\ell(x_2)\|,$$

and we have that

$$\|J_\ell(x)\| \|\epsilon\| \geq \|F_\ell(x) - F_\ell(x_{adv})\| \geq \eta_\ell(F). \quad (2)$$

Combining (2) and (1) (and ignoring the Taylor approximation error), we lower bound the norm of the distortion ϵ in terms of the embedding margin and the norm of the Jacobian,

$$\|\epsilon\| \geq \frac{\eta_\ell(F)}{\|J_\ell(x)\|}. \quad (3)$$

While the attacker’s goal is to find a small distortion leading to misclassification, our goal as the defender is to create a resilient model that forces a maximal distortion. We refer to (3) as the *maximal adversarial distortion* (MAD) principle. The MAD strategy is thus to explicitly maximize the right-hand side of (3) with respect to the embedding layer of the model F . To successfully do so, we must increase the embedding margin $\eta_\ell(F)$ while decreasing the norm of the Jacobian $\|J_\ell(x)\|$. Thus, the MAD principle tells us that the embedding margin must be measured in terms of gradient units (gradients of the model with respect to the input), and it is meaningless to enlarge the embedding margin alone without bounding the Jacobian.

3 Increasing Resiliency with MAD Optimization

In this section we describe the MAD optimization technique, which includes the MAD loss function and training routine. The MAD loss function (presented below) is applied to the final embedding layer of a given network F . We note that, technically, we can also apply the MAD procedure to any other layer in the model (or several layers simultaneously), but defer such explorations to future work.

To apply the MAD principle (3), need increase the embedding margin $\eta_\ell(F)$ and decrease the Jacobian norm $\|J_\ell(x)\|$. We achieve the first objective by adopting ideas from classical cluster analysis. Specifically, we observe that the increase in the embedding margin, $\eta_\ell(F)$, can be accomplished by increasing the distance between clusters and reducing their variance. Let $\mu_c = \frac{1}{N_c} \sum_{i=1}^{N_c} \mathbf{z}_i^c$ be the mean of each cluster, where N_c is the number of samples from class c and \mathbf{z}_i^c is the embedding vector of sample i from class c , and let M be the number of classes. We have that,

$$\begin{aligned} \text{Cluster Variance} &\triangleq \sum_{c=1}^M \frac{1}{N_c} \sum_{i=1}^{N_c} \|\mathbf{z}_i^c - \mu_c\|_2 \\ \text{Cluster Distance} &\triangleq \frac{1}{M} \sum_{c=1}^M \frac{1}{M-1} \sum_{i \neq c}^M \|\mathbf{z}_i - \mu_c\|_2. \end{aligned}$$

To increase the margin, we would like to minimize the following objective,

$$\text{Margin Objective} = \text{Cluster Variance} - \text{Cluster Distance}.$$

Unlike the cluster variance, maximization of the cluster distance is problematic because the distance is potentially unbounded. We can, however, proxy this quantity using the angular distance between clusters, which is bounded. To this end, we use the cosine similarity and utilize a Siamese training procedure, as described in Section 3.1.

3.1 MAD Optimization Components

To explicitly increase the embedding margin, we propose using **Siamese training** as follows. We create a Siamese network Bromley et al. [1994], where each subnetwork is our classifier F . The Siamese network receives two input instances denoted by $x_i^c, x_j^{\tilde{c}}$, and generates three outputs: two classification outputs and one auxiliary output for the cosine similarity between each subnetwork’s embedding. We introduce an additional loss term to force embeddings from different class samples to have a cosine similarity of 0 (and 1 otherwise). Formally,

$$\text{SiameseLoss} \triangleq \frac{\mathbf{z}_i^c \cdot \mathbf{z}_j^{\tilde{c}}}{\|\mathbf{z}_i^c\| \|\mathbf{z}_j^{\tilde{c}}\|} = \begin{cases} 1, & \text{if } c = \tilde{c}; \\ 0, & \text{else.} \end{cases}$$

Inspired by Szegedy et al. [2016], we include an additional loss term that penalizes each class cluster individually for large variance. We refer to this component as the “**reduce variance loss**” (RVL). Formally,

$$\sigma_c \triangleq \frac{1}{N_c} \sum_{i=1}^{N_c} \|\mathbf{z}_i^c - \boldsymbol{\mu}_c\|_2, \quad \text{RVL} \triangleq \frac{1}{N_c} \sum_{c=1}^{N_{\text{classes}}} \sigma_c. \quad (4)$$

The variance is estimated per class on each mini-batch, then averaged and minimized as part of the learning process.

Finally, we add a **Jacobian reduction loss**, which explicitly evaluates the Jacobian per mini-batch, and include its norm in the DNN’s loss function. Formally, $J_\ell(x) = \frac{\partial F_\ell(x)}{\partial x}$, where the derivative is taken for each input in a mini-batch. To minimize the norm of the Jacobian, we include it in the MAD loss function.

3.2 Training with MAD Optimization

A simultaneous application of all components described above is obtained using the following MAD loss function, denoted \mathcal{L}_{MAD} ,

$$\begin{aligned} \mathcal{L}_{MAD}(x_1, x_2, y_1, y_2; F) &\triangleq \lambda_{\text{CE}} \text{CE}(x_1, y_1; F) + \lambda_{\text{CE}} \text{CE}(x_2, y_2; F) \\ &+ \lambda_{\text{Siam}} \left(\delta_{y_1, y_2} - \frac{\mathbf{z}_1 \mathbf{z}_2}{\|\mathbf{z}_1\| \|\mathbf{z}_2\|} \right)^2 \\ &+ \lambda_{\text{RVL}} \frac{1}{N_c} \sum_{c=1}^{N_{\text{classes}}} \sigma_c(x_1) + \lambda_{\text{RVL}} \frac{1}{N_c} \sum_{c=1}^{N_{\text{classes}}} \sigma_c(x_2) \\ &+ \lambda_{\text{Jacob}} \left\| \frac{\partial F(x_1)}{\partial x_1} \right\| + \lambda_{\text{Jacob}} \left\| \frac{\partial F(x_2)}{\partial x_2} \right\|, \end{aligned}$$

where $\text{CE}(x, y; F)$ is the cross-entropy loss of x given its label y , and $\lambda_{\text{CE}}, \lambda_{\text{RVL}}, \lambda_{\text{Siam}}$, and λ_{Jacob} are hyperparameters (taken in our experiments to be 1, 1, 1, 0.01, respectively).¹ In addition, we require a specialized mini-batch construction procedure. A pseudo-code of the training procedure is given in Algorithm 1 in Appendix B. The code is self-explanatory for the most part. We note, however, that an epoch begins by creating a Siamese counterpart for each instance–label pair in a given batch. With probability Q , the Siamese sample is selected from the same class, and its cosine similarity label is set to 1. Otherwise (probability $1 - Q$), the Siamese sample is selected from a different class, and its cosine similarity label is set to 0. Both target classes’ activation is set to α , a label smoothing hyperparameter (see Appendix F). Notice that the Siamese, RVL and Jacobian norm (Equation 4) components are computed from the embedding vectors of each mini-batch.

¹ $\lambda_{\text{Jacob}} = 0.01$ was chosen to make this component roughly of the same magnitude as the other components.

4 Related Work

Many interesting ideas have been proposed to construct defense mechanisms against adversarial examples. These can be broadly divided into two categories. The first are *active* algorithms that process the input or output of the DNN at prediction time, removing the effects of the adversarial algorithm. Amongst these algorithms are: Neural Fingerprinting Dathathri et al. [2018], that transforms the DNN’s input such that a specific, pre-defined prediction is expected; Stochastic Adversarial Pruning Dhillon et al. [2018], that adds a randomized, dropout-like mechanism to the prediction process; and others. The second category, to which the algorithm presented in this paper belongs, is that of *passive* defense algorithms. Such algorithms alter the DNN’s training process, loss function or architecture to create a network that is more robust to adversarial attacks. One popular passive approach is adversarial training Goodfellow et al. [2014], Madry et al. [2017], Yan et al. [2018], where adversarial examples are introduced during the training procedure, making the DNN more robust to perturbations in the input instance. Another approach is the ensemble approach Tramèr et al. [2017], Strauss et al. [2017], Pang et al. [2019] where, instead of training a single predictor, the training process includes several different DNNs, all trained together with a single loss function that collects the predictions.

A formal approach to adversarial defense is the *certification approach* Hein and Andriushchenko [2017], which is designed to provide a lower bound for the penetration distortion attempting to fool a given network. Certified defense methods are referred to as being either “exact” or “conservative”. In exact methods, no distortion smaller than the certification bound can penetrate or confuse the DNN Hein and Andriushchenko [2017], Wong and Kolter [2017], Wong et al. [2018], Cohen et al. [2019]. In conservative methods, the bound is merely a relative metric for comparing DNN robustness to adversarial examples Ding et al. [2018], Tsuzuku et al. [2018], Zhang et al. [2019]. Both exact and conservative methods have been criticized for being computationally expensive and unscalable. Tjeng et al. [2018], Cohen et al. [2019]. Moreover, so far these techniques have lacked in performance. In contrast, our pragmatic approach that relies on a lower bound approximation, does not provide a theoretical guarantee but leads to excellent performance.

Improving the separability of the class clusters in the intermediate layers of a DNN as a mean of defending against adversarial attack is a notion established by Hein and Andriushchenko [2017]. Following their work, many defense methods have been suggested to increase the margin between classes while maintaining a feasible training process so as to be applicable to large-scale DNNs. Liu et al. [2016] and Wang et al. [2018] added an angular constraint to the loss function, forcing a large angular distance between classes. Elsayed et al. [2018] suggested a margin increasing loss function that explicitly aims to increase the distance between class clusters, truncating the maximal distance given that increasing the distance is an unbounded term. Mustafa et al. [2019] suggested arranging the features of each class in specific convex polytopes. To that end, they employed an auxiliary loss function based on the distance between instance features and a p -norm ball around the class centroid. Chan et al. [2019] presented the Jacobian Adversarially Regularized Networks (JARN) method in which they imposed constraints on the DNN’s Jacobian and showed their impact on the DNN’s robustness to adversarial attacks. In contrast, our MAD principle (Section 2) states that separability and Jacobian must be optimized together so that separability is gradient-normalized, and it is sub-optimal to consider each of these quantities individually.

5 Experimental Evaluation

We now evaluate the merit of our MadNet approach as a defence mechanism against adversarial attacks. We start by describing the experimental setup, including the precise specification of what the adversary knows and can do. We then present qualitative insight on the embedding separability of MadNets, followed by detailed quantitative evaluation in the face of varied attacks.

5.1 Experimental Setup

Following Mustafa et al. [2019], Pang et al. [2019], Chan et al. [2019], Elsayed et al. [2018], we evaluated MadNet on three image datasets: MNIST LeCun et al. [1998], CIFAR-10 and CIFAR-100 Krizhevsky and Hinton [2009]. We tested four different attacks: *FGSM*, *BIM*, *PGD* and *C&W*. For PGD and BIM we used 10 iterations and several values of the maximal L_∞ perturbation ϵ , in line with the perturbation used by the baseline Mustafa et al. [2019]. A detailed description of the different attacks can be found in Appendix D. We chose ResNet-56 He et al. [2016] as the backbone architecture of MadNet. A full description of the training parameters can be found in Appendix C. We compare our results to the vanilla ResNet-56 baseline trained with cross-entropy, denoted as *CE*, and to robustness results presented by Mustafa et al. [2019]. In their work, they conducted a thorough ablation study and were able to surpass Madry et al. [2017], Yu et al. [2018], Kurakin et al. [2016b], Ross and Doshi-Velez [2018]. As such, we consider their work as the current state-of-the-art, under a similar threat model and test for the attacks and under the same parameter setting as in their ablation study. For the C&W attack we used 1000 iterations with the confidence set to 0 and various

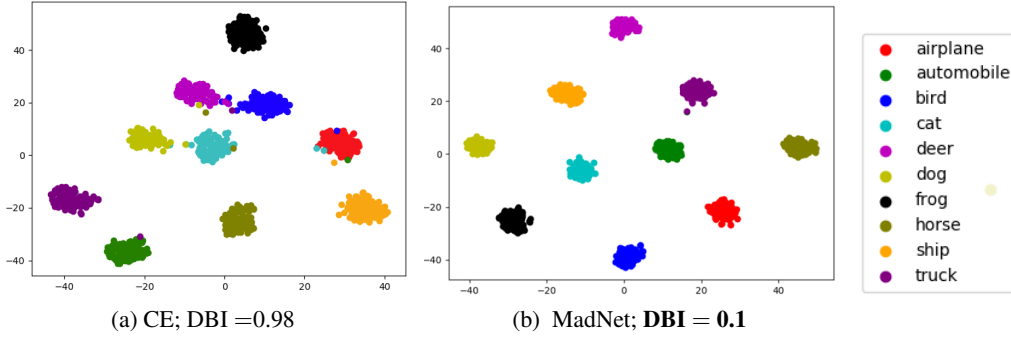


Figure 2: CIFAR-10 t-SNE and Davies–Bouldin Index (DBI) for CE and MadNet.

values of the initial constant c . We also apply a maximal L_∞ perturbation as done by Mustafa et al. [2019], setting the maximal perturbation to 0.3 for MNIST and 0.03 for CIFAR-10 and CIFAR-100. Results are reported as the accuracy, in percentage, on 1000 adversarially perturbed images, taken from the test set, which were correctly classified prior to the perturbation.

To evaluate a defense algorithm’s efficiency against these adversarial attacks, we consider two threat models, differentiated by the knowledge the adversary has of the classifier (target network) and the defense mechanism being used.

Black-Box Threat Model: In this model, the adversary has no knowledge of our system. It does not know the target network architecture, cannot access its gradients and does not know the defense methods. The adversary can, however, sample the target network for input-output pairs and has access to the dataset used to train the target network.

White-Box Threat Model: In this model, we assume the adversary has full knowledge of the entire system to be attacked, and can access its gradients to produce the adversarial example. We tested the black-box and white-box threat models on each dataset.

5.2 Qualitative Observations on Embedding Separability

Using t-SNE Maaten and Hinton [2008] to visualize the embedding space activations, Figure 2 illustrates how MAD optimization affects the separability of class embedding clusters. Figure 2a depicts class clusters in the embedding layer after standard training over CIFAR-10 (without MAD). Figure 2b shows the clusters obtained when using a complete MAD optimization, which also includes Jacobian reduction. We note that t-SNE is mainly useful for visualization and can often distort the overall relationships in high dimensions. To obtain a reliable ablation study, we calculated the Davies–Bouldin index (DBI) Davies and Bouldin [1979], which is frequently used to evaluate clustering quality according to the distance between cluster centroids divided by the Euclidean distance between points within a cluster (a lower score means better clustering). DBI scores are shown for all four embedding clusterings in Figure 2. It is evident that each MAD optimization component contributes significantly to separability, and the DBI of a complete MAD optimization is the best by far.

5.3 White-Box Study

For the white-box threat model we consider MadNet with two training procedures. The first is where only normal samples are introduced during the training process. The second is adversarial training where we use the PGD attack during the training of MadNet, and introduce adversarial examples in the training process. Results for the white-box threat model appear in Table 1, Table 2, and Table 3, with the best method without adversarial training highlighted in green, and the best method with adversarial training in blue. Examining these tables, we first note that MadNet does not significantly degrade the performance on normal instances and even improves it for CIFAR-10 (first row in the table). It is evident that MadNet outperforms the competition on the vast majority of the scenarios tested, especially when using adversarial training, improving the results even for attacks not introduced during training. Moreover, MadNet’s performance on MNIST with adversarial training displays near perfect results, creating an almost impenetrable model. MadNet’s performance on CIFAR-10 and CIFAR-100 indicates that it is appropriate for more complex images than MNIST as well as for a larger number of classes. We note that the significantly better performance for higher-constant C&W is partially caused by the L_∞ bound imposed. When the L_∞ constraint is removed, MadNet achieves an accuracy

of 71.6% with adversarial training and 67.2% without for MNIST with $c = 10$, and 61.5% with adversarial training for CIFAR-10 with $c = 0.1$. Other C&W scenarios were not significantly affected by this constraint.

Table 1: MNIST adversarial robustness (%) under the white-box threat model.

Attack	CE	Mustafa et al.	MadNet	Mustafa et al. Adv training	MadNet Adv training
No Attack	99.22	99.5	99.3	99.3	99.3
C&W ($c = 0.1$)	31.6	97.7	98.3	97.6	99.4
C&W ($c = 1$)	0	80.4	93.1	91.2	98.1
C&W ($c = 10$)	0	29.1	92.5	46.0	97.9
FGSM($\epsilon = 0.1$)	74	97.1	95.3	96.5	98.3
FGSM($\epsilon = 0.2$)	23	70.6	73.5	77.9	95.8
BIM($\epsilon = 0.1$)	17.4	90.2	92.2	92.1	98.6
BIM($\epsilon = 0.15$)	3.4	70.6	87	77.3	95.2
PGD ($\epsilon = 0.1$)	10.6	83.6	92.4	93.9	98.8
PGD ($\epsilon = 0.15$)	0.6	62.5	83.4	80.2	98.4

Table 2: CIFAR-10 adversarial robustness (%) under the white-box threat model.

Attack	CE	Mustafa et al.	MadNet	Mustafa et al. Adv training	MadNet Adv training
No-Attack	93	90.5	94.2	91.9	92.1
CW ($c = 0.001$)	30.5	84.3	79.3	91.3	93.4
CW ($c = 0.01$)	0	63.5	68.5	73.7	92.4
CW ($c = 0.1$)	0	41.1	63.7	60.5	81.2
FGSM($\epsilon = 0.02$)	23.5	72.5	70.6	78.5	76.1
FGSM($\epsilon = 0.04$)	16.3	56.3	63.3	69.9	70.3
BIM($\epsilon = 0.01$)	0	62.9	68.4	74.5	77.2
BIM($\epsilon = 0.02$)	0	40.1	53.4	57.3	54.8
PGD ($\epsilon = 0.01$)	0	60.1	68.8	75.7	85
PGD ($\epsilon = 0.02$)	0	39.3	55.2	58.5	60.2

Table 3: CIFAR-100 adversarial robustness (%) under the white-box threat model.

Attack	CE	Mustafa et al.	MadNet	Mustafa et al. Adv training	MadNet Adv training
No-Attack	72.3	71.9	71.1	68.3	66.7
BIM($\epsilon = 0.005$)	4	44.8	46.8	55.7	78.1
BIM($\epsilon = 0.01$)	1	39.8	31.2	46.9	62.8
PGD ($\epsilon = 0.005$)	8	42.2	53.4	55	76
PGD ($\epsilon = 0.01$)	1	38.9	33.5	44	63.1

5.4 Black-Box Study

To evaluate our model in the black-box threat model, where the attacker cannot access the model’s weights, we followed Papernot et al. [2017], Carlini et al. [2019] and created a proxy model, which was trained using input-output pairs probed from the defender’s (target) model (i.e., the proxy model was trained via teacher-student distillation of the target model). The proxy model was then used by the attacker to generate adversarial examples under the *white-box* threat model. These adversarial examples were then tested against the target model. The proxy model we chose was ResNet-32. One main purpose of the black-box threat model is to check for obfuscated gradients. In their paper, Athalye et al. [2018] listed defense methods that mask or obstruct the DNN’s gradients. As such, when the attacking algorithms attempts to create an adversarial example it fails to do so, simply because of its inability to properly derive the DNN’s output w.r.t its input. This might give a false sense of security since with slight modifications of the attacks, these defenses can be overcome. If a defense method performs better under the white-box threat model, this would indicate an obfuscation of gradients. The adversarial robustness results under the black-box threat model appear in Table 4. As expected, the black-box threat model’s performance is superior to that of the white-box threat model achieving, for example, 97.6%, 95.7% and 78.3% against the black-box PGD attack on MNIST, CIFAR-10 and CIFAR-100 respectively vs 92.4%,

Table 4: Adversarial robustness (%) for MadNet under the black-box threat model.

Attack	MNIST	CIFAR-10	CIFAR-100
	$\epsilon = 0.1, c = 0.1$	$\epsilon = 0.02, c = 0.001$	$\epsilon = 0.01$
CE			
FGSM	74.2	51.3	61.5
BIM	81.7	49.1	44.3
PGD	78.3	57.8	47.2
C&W	94.3	92.3	95.2
MAD			
FGSM	98.1	85.1	80.8
BIM	98	96.3	79.8
PGD	97.6	95.7	78.3
C&W	100	100	98

68.8 and 33.5% against its white-box counterpart. While this alone does not guarantee the gradients are not masked or manipulated, we argue that the components that constitute the MAD loss do not impose any constraints on the model’s gradients other than the derivation for the Jacobian reduction, a process that also occurs when performing standard adversarial training.

6 Conclusions

We introduced maximum adversarial distortion (MAD), a powerful approach for the defense of deep models against adversarial attacks by optimizing for sensitivity-normalized embedding separability. We demonstrated state-of-the-art results in defending against adversarial attacks. In addition, we provided some geometric intuition on attacks and defenses using both Davies–Bouldin Index analysis and t-SNE visualizations. This work raises several interesting questions. First, it would be valuable to examine other methods for margin maximization and Jacobian reduction. For example, a recent work by Zhang et al. [2019] proposed an iterative technique to reduce the norm of the Jacobian. In addition, it would also be interesting to explore ways to increase the margin (and reduce the Jacobian) on shallower embedding layers where lower-level features are formed. Finally, our MAD approach utilized a first-order approximation and ignored the Taylor approximation error term, which can be bounded in terms of $\|H_\ell(x)\|$ and $\|\epsilon\|^2$, where H_ℓ is the Hessian of the embedding layer with respect to the input. It would be valuable to try and further robustify networks by also accounting for this error term.

Broader Impact

In this paper we present a strong defense method against adversarial attacks. As such, the paper potentially has a positive societal effect because defense techniques constitute our only countermeasure against malicious attempts to fool deep learning systems that help or serve the public. We are unable to identify negative consequences of the proposed algorithms.

References

- A. Athalye, N. Carlini, and D. Wagner. Obfuscated gradients give a false sense of security: Circumventing defenses to adversarial examples. *arXiv preprint arXiv:1802.00420*, 2018.
- J. Bromley, I. Guyon, Y. LeCun, E. Säcker, and R. Shah. Signature verification using a " siamese" time delay neural network. In *Advances in neural information processing systems*, pages 737–744, 1994.
- N. Carlini and D. Wagner. Adversarial examples are not easily detected: Bypassing ten detection methods. In *Proceedings of the 10th ACM Workshop on Artificial Intelligence and Security*, pages 3–14. ACM, 2017a.
- N. Carlini and D. Wagner. Towards evaluating the robustness of neural networks. In *2017 IEEE Symposium on Security and Privacy (SP)*, pages 39–57. IEEE, 2017b.
- N. Carlini, A. Athalye, N. Papernot, W. Brendel, J. Rauber, D. Tsipras, I. Goodfellow, and A. Madry. On evaluating adversarial robustness. *arXiv preprint arXiv:1902.06705*, 2019.

- A. Chan, Y. Tay, Y. S. Ong, and J. Fu. Jacobian adversarially regularized networks for robustness. *arXiv preprint arXiv:1912.10185*, 2019.
- J. M. Cohen, E. Rosenfeld, and J. Z. Kolter. Certified adversarial robustness via randomized smoothing. *arXiv preprint arXiv:1902.02918*, 2019.
- S. Dathathri, S. Zheng, R. M. Murray, and Y. Yue. Detecting adversarial examples via neural fingerprinting. *arXiv preprint arXiv:1803.03870*, 2018.
- D. L. Davies and D. W. Bouldin. A cluster separation measure. *IEEE transactions on pattern analysis and machine intelligence*, (2):224–227, 1979.
- G. S. Dhillon, K. Azizzadenesheli, Z. C. Lipton, J. Bernstein, J. Kossaifi, A. Khanna, and A. Anandkumar. Stochastic activation pruning for robust adversarial defense. *arXiv preprint arXiv:1803.01442*, 2018.
- G. W. Ding, Y. Sharma, K. Y. C. Lui, and R. Huang. Max-margin adversarial (mma) training: Direct input space margin maximization through adversarial training. *arXiv preprint arXiv:1812.02637*, 2018.
- G. Elsayed, D. Krishnan, H. Mobahi, K. Regan, and S. Bengio. Large margin deep networks for classification. In *Advances in neural information processing systems*, pages 842–852, 2018.
- I. J. Goodfellow, J. Shlens, and C. Szegedy. Explaining and harnessing adversarial examples. *arXiv preprint arXiv:1412.6572*, 2014.
- K. He, X. Zhang, S. Ren, and J. Sun. Deep residual learning for image recognition. In *Proceedings of the IEEE conference on computer vision and pattern recognition*, pages 770–778, 2016.
- M. Hein and M. Andriushchenko. Formal guarantees on the robustness of a classifier against adversarial manipulation. In *Advances in Neural Information Processing Systems*, pages 2266–2276, 2017.
- E. Hoffer and N. Ailon. Deep metric learning using triplet network. In *International Workshop on Similarity-Based Pattern Recognition*, pages 84–92. Springer, 2015.
- A. Krizhevsky and G. Hinton. Learning multiple layers of features from tiny images. Technical report, Citeseer, 2009.
- A. Kurakin, I. Goodfellow, and S. Bengio. Adversarial examples in the physical world. *arXiv preprint arXiv:1607.02533*, 2016a.
- A. Kurakin, I. Goodfellow, and S. Bengio. Adversarial machine learning at scale. *arXiv preprint arXiv:1611.01236*, 2016b.
- Y. LeCun, L. Bottou, Y. Bengio, P. Haffner, et al. Gradient-based learning applied to document recognition. *Proceedings of the IEEE*, 86(11):2278–2324, 1998.
- X. Liang, X. Wang, Z. Lei, S. Liao, and S. Z. Li. Soft-margin softmax for deep classification. In *International Conference on Neural Information Processing*, pages 413–421. Springer, 2017.
- W. Liu, Y. Wen, Z. Yu, and M. Yang. Large-margin softmax loss for convolutional neural networks. In *ICML*, volume 2, page 7, 2016.
- L. v. d. Maaten and G. Hinton. Visualizing data using t-sne. *Journal of machine learning research*, 9(Nov):2579–2605, 2008.
- A. Madry, A. Makelov, L. Schmidt, D. Tsipras, and A. Vladu. Towards deep learning models resistant to adversarial attacks. *arXiv preprint arXiv:1706.06083*, 2017.
- R. Müller, S. Kornblith, and G. Hinton. When does label smoothing help? *arXiv preprint arXiv:1906.02629*, 2019.
- A. Mustafa, S. Khan, M. Hayat, R. Goecke, J. Shen, and L. Shao. Adversarial defense by restricting the hidden space of deep neural networks. In *Proceedings of the IEEE International Conference on Computer Vision*, pages 3385–3394, 2019.
- T. Pang, K. Xu, C. Du, N. Chen, and J. Zhu. Improving adversarial robustness via promoting ensemble diversity. *arXiv preprint arXiv:1901.08846*, 2019.

- N. Papernot, P. McDaniel, X. Wu, S. Jha, and A. Swami. Distillation as a defense to adversarial perturbations against deep neural networks. In *2016 IEEE Symposium on Security and Privacy (SP)*, pages 582–597. IEEE, 2016.
- N. Papernot, P. McDaniel, I. Goodfellow, S. Jha, Z. B. Celik, and A. Swami. Practical black-box attacks against machine learning. In *Proceedings of the 2017 ACM on Asia conference on computer and communications security*, pages 506–519. ACM, 2017.
- A. S. Ross and F. Doshi-Velez. Improving the adversarial robustness and interpretability of deep neural networks by regularizing their input gradients. In *Thirty-second AAAI conference on artificial intelligence*, 2018.
- J. Sokolić, R. Giryes, G. Sapiro, and M. R. Rodrigues. Robust large margin deep neural networks. *IEEE Transactions on Signal Processing*, 65(16):4265–4280, 2017.
- T. Strauss, M. Hanselmann, A. Junginger, and H. Ulmer. Ensemble methods as a defense to adversarial perturbations against deep neural networks. *arXiv preprint arXiv:1709.03423*, 2017.
- S. Sun, W. Chen, L. Wang, X. Liu, and T.-Y. Liu. On the depth of deep neural networks: A theoretical view. In *Thirtieth AAAI Conference on Artificial Intelligence*, 2016.
- C. Szegedy, W. Zaremba, I. Sutskever, J. Bruna, D. Erhan, I. Goodfellow, and R. Fergus. Intriguing properties of neural networks. *arXiv preprint arXiv:1312.6199*, 2013.
- C. Szegedy, V. Vanhoucke, S. Ioffe, J. Shlens, and Z. Wojna. Rethinking the inception architecture for computer vision. In *Proceedings of the IEEE conference on computer vision and pattern recognition*, pages 2818–2826, 2016.
- V. Tjeng, K. Y. Xiao, and R. Tedrake. Evaluating robustness of neural networks with mixed integer programming. 2018.
- F. Tramèr, A. Kurakin, N. Papernot, I. Goodfellow, D. Boneh, and P. McDaniel. Ensemble adversarial training: Attacks and defenses. *arXiv preprint arXiv:1705.07204*, 2017.
- Y. Tsuzuku, I. Sato, and M. Sugiyama. Lipschitz-margin training: Scalable certification of perturbation invariance for deep neural networks. In *Advances in Neural Information Processing Systems*, pages 6541–6550, 2018.
- H. Wang, Y. Wang, Z. Zhou, X. Ji, D. Gong, J. Zhou, Z. Li, and W. Liu. Cosface: Large margin cosine loss for deep face recognition. In *Proceedings of the IEEE Conference on Computer Vision and Pattern Recognition*, pages 5265–5274, 2018.
- Y. Wen, K. Zhang, Z. Li, and Y. Qiao. A discriminative feature learning approach for deep face recognition. In *European conference on computer vision*, pages 499–515. Springer, 2016.
- E. Wong and J. Z. Kolter. Provable defenses against adversarial examples via the convex outer adversarial polytope. *arXiv preprint arXiv:1711.00851*, 2017.
- E. Wong, F. Schmidt, J. H. Metzen, and J. Z. Kolter. Scaling provable adversarial defenses. In *Advances in Neural Information Processing Systems*, pages 8400–8409, 2018.
- Z. Yan, Y. Guo, and C. Zhang. Deep defense: Training dnns with improved adversarial robustness. In *Advances in Neural Information Processing Systems*, pages 417–426, 2018.
- F. Yu, C. Liu, Y. Wang, L. Zhao, and X. Chen. Interpreting adversarial robustness: A view from decision surface in input space. *arXiv preprint arXiv:1810.00144*, 2018.
- H. Zhang, P. Zhang, and C.-J. Hsieh. Recurjac: An efficient recursive algorithm for bounding jacobian matrix of neural networks and its applications. In *Proceedings of the AAAI Conference on Artificial Intelligence*, volume 33, pages 5757–5764, 2019.

Appendices

A L_2 Norm Sub-Multiplicativity

Given $A \in \mathbb{R}^{N \times M \times K}$ and $B \in \mathbb{R}^{K \times J \times L}$, we claim that the Frobenius norm of the multiplication of A and B is less than or equal to the multiplication of each tensor's Frobenius norm. Proof:

$$\begin{aligned}
 \|AB\|_F^2 &= \sum_{n=1}^N \sum_{m=1}^M \sum_{j=1}^J \sum_{l=1}^L \left| \sum_{k=1}^K a_{n,m,k} b_{k,j,l} \right|^2 \\
 &\leq \sum_{n=1}^N \sum_{m=1}^M \sum_{j=1}^J \sum_{l=1}^L \sum_{k=1}^K |a_{n,m,k}|^2 \sum_{k=1}^K |b_{k,j,l}|^2 && \text{(Cauchy-Schwarz)} \\
 &= \sum_{n=1}^N \sum_{m=1}^M \sum_{j=1}^J \sum_{l=1}^L \left(\sum_{k=1}^K |a_{n,m,k}|^2 |b_{k,j,l}|^2 \right) \\
 &= \sum_{n=1}^N \sum_{m=1}^M \sum_{k=1}^K |a_{n,m,k}|^2 \sum_{j=1}^J \sum_{l=1}^L \sum_{s=1}^K |b_{s,j,l}|^2 && (5) \\
 &= \|A\|_F^2 \|B\|_F^2
 \end{aligned}$$

B MAD Algorithm

The MAD algorithm appears in Algorithm 1.

C Classifier Hyperparameters

Parameter	Value
Optimizer	SGD
ResNet Depth	56
Weight Regularization	L2 (0.002)
Batch Size	128
Initial Learning Rate	0.1
Epochs-CIFAR-10	400
Epochs-MNIST	80
Activation	Leaky-Relu (0.1)
λ_{CE}	1
λ_{siam}	1
λ_{RVL}	1
$\lambda_{\text{Jacobian}}$	0.01
α	0.8

D Adversarial Attacks

We use various attack algorithms to evaluate our defense method. We denote x, x' as the input and adversarial instance, respectively, ℓ as the target label, F as the target model with loss function $L_F(x, \ell)$ and $\epsilon = \|x - x'\|$ as the pixel-wise perturbation between the adversarial and normal instances. The general formulation, therefore, becomes,

$$\underset{x'}{\text{minimize}} \|x - x'\|^2 \quad \text{s.t.} \quad F(x') = \ell. \quad (6)$$

FGSM: Goodfellow et al. [2014] introduced the fast gradient sign method (FGSM), which optimizes the adversarial instance by back-propagating the input through the attacked DNN, in accordance with the desired target. Formally,

Algorithm 1 MadNet optimization

```

1: procedure MAD
2:   for batch = 1, . . . , #batches do
3:      $X, Y \leftarrow \text{get\_batch}()$ 
4:     initialize  $X_{\text{siamese}} = [], Y_{\text{siamese}} = [], S = []$ 
5:     for  $b = 1, \dots, \text{batch\_size}$  do
6:        $q \sim \text{Bernoulli}(Q)$ 
7:       if  $q == 1$  then
8:          $y \leftarrow Y[b]$ 
9:          $s \leftarrow 1$ 
10:      else
11:         $y \leftarrow \text{random class} \neq y_1$ 
12:         $s \leftarrow 0$ 
13:      end if
14:       $x \leftarrow \text{random sample from class } Y[b]$ 
15:      Append  $x, y, s$  to  $X_{\text{siamese}}, Y_{\text{siamese}}, S$ 
16:    end for
17:     $z_1, z_2 \leftarrow F_\ell(X), F_\ell(X_{\text{siamese}})$  ▷ embedding
18:     $p_1, p_2 \leftarrow F(X), F(X_{\text{siamese}})$  ▷ logits
19:     $SL = \frac{1}{\text{batch\_size}} \sum | \frac{z_1 z_2}{\|z_1\| \|z_2\|} - S |$ 
20:     $RVL \leftarrow 0$ 
21:     $JL \leftarrow \left\| \frac{\partial F(x_1)}{\partial x_1} \right\| + \left\| \frac{\partial F(x_2)}{\partial x_2} \right\|$ 
22:    for  $c = 0, \dots, M$  do
23:       $\mu_c = \frac{1}{N_c} \sum_{i=1}^{N_c} z_i^c$ 
24:       $\sigma_c = \frac{1}{N_c} \sum_{i=1}^{N_c} \|z_i^c - \mu_c\|_2$ 
25:       $RVL \leftarrow RVL + \sigma_c$ 
26:    end for
27:    minimize  $\mathcal{L}_{MAD}$ 
28:  end for
29: end procedure

```

letting ϵ be a fixed parameter, the adversarial example is,

$$x' = x + \epsilon \text{sign}(\nabla L_F(x, \ell)). \quad (7)$$

While not as effective as other attack algorithms, this method has the advantage of being one of the fastest ones.

BIM: Kurakin et al. [2016a] introduced the Basic Iterative Method (BIM), which performs the FGSM method iteratively, clipping the perturbation if needed. Formally,

$$x'_{N+1} = x'_N + \epsilon \text{sign}(\nabla L_F(x'_N, l)),$$

where ϵ is a fixed parameter.

PGD: Madry et al. [2017] proposed an attack similar to BIM, performing FGSM steps from a sample randomly selected from a neighbourhood of x .

C&W: Carlini and Wagner [2017b] introduced the C&W method, which operates by modifying the L-BFGS method as follows,

$$\underset{x'}{\text{minimize}} \|x - x'\|^2 + cf(x'),$$

where c is a hyperparameter and the loss function, f , is chosen such that $f(x') \leq 0$ if x' is classified as the target class; namely,

$$f(x') = \max(Z(x')_\ell - Z(x')_t, \kappa)$$

where Z is the target DNN logits, t is the correct label and κ is a hyperparameter referring to the confidence of the attack. The higher the confidence, the higher the activation for the target class is, and therefore, the larger the perturbation. Three different Euclidean norms are considered with this algorithm, L_0, L_2, L_∞ . We conduct our evaluation using L_2 . This attack method is considered very effective and has had great success in overcoming various defense methods Papernot et al. [2016], Carlini and Wagner [2017b].

E Adversarial Attack Parameters

The parameters chosen to create the adversarial examples per attack are given in Table 5.

Table 5: Adversarial attack parameters.

Attack	Parameter	Value
BIM	Iterations	10
PGD	Iterations	10
CW	Max Iterations	1000
	Binary Search Steps	1
	Confidence	0

F Label Smoothing

Label smoothing, the process of training a DNN with soft labels rather than a one-hot vector, has been shown to decrease the gradients w.r.t. the model’s weights Müller et al. [2019], while not directly used in the context of adversarial robustness. Intuitively, the “cost” of an incorrect prediction is lower when the target label’s activation is lower than 1. As such, the update increment of the weights is lower than in standard one-hot training. By the same logic, if we consider the weights fixed and the input instance as being updated according to a gradient step, as is the basis of adversarial attacks, we can deduce that the gradients will be lower than those of a standard training procedure. We set the softmax response of the correct class to α and the remaining classes are distributed evenly to sum to 1.